Cloning and characterization of a novel human histone deacetylase, HDAC8

Joseph J. BUGGY[1], Mindy L. SIDERIS, Polly MAK, Donald D. LORIMER[2], Brian McINTOSH[3] and James M. CLARK
AXYS Pharmaceuticals, 180 Kimball Way, South San Francisco, CA 94080, U.S.A.

Histone deacetylases (HDACs) are a growing family of enzymes implicated in transcriptional regulation by affecting the acetylation state of core histones in the nucleus of cells. HDACs are known to have key roles in the regulation of cell proliferation [Brehm, Miska, McCance, Reid, Bannister and Kouzarides (1998) Nature (London) **391**, 597–600], and aberrant recruitment of an HDAC complex has been shown to be a key step in the mechanism of cell transformation in acute promyelocytic leukaemia [Grignani, De Matteis, Nervi, Tomassoni, Gelmetti, Cioce, Fanelli, Ruthardt, Ferrara, Zamir et al. (1998) Nature (London) **391**, 815–818; Lin, Nagy, Inoue, Shao, Miller and Evans (1998), Nature (London) **391**, 811–814]. Here we present the complete nucleotide sequence of a cDNA clone, termed HDAC8, that encodes a protein product with similarity to the RPD3 class (I) of HDACs. The predicted 377-residue HDAC8 product contains a shorter C-terminal extension relative to other members of its class. After expression in two cell systems, immunopurified HDAC8 is shown to possess trichostatin A- and sodium butyrate-inhibitable HDAC activity on histone H4 peptide substrates as well as on core histones. Expression profiling reveals the expression of HDAC8 to various degrees in every tissue tested and also in several tumour lines. Mutation of two adjacent histidine residues within the predicted active site severely decreases activity, confirming these residues as important for HDAC8 enzyme activity. Finally, linkage analysis after radiation hybrid mapping has localized HDAC8 to chromosomal position Xq21.2–Xq21.3. These results confirm HDAC8 as a new member of the HDAC family.

Key words: acetylation, histone H4, trichostatin A.

INTRODUCTION

Modification of chromatin structure via the reversible acetylation of nucleosomal histones is important in the regulation of transcription in eukaryotic cells (reviewed in [1]). Acetylation of the ϵ-amino group of specific lysine residues within the N-terminal tail of core histones results in localized chromatin relaxation. This acetylation is required to maintain the unfolded structure of nucleosomes undergoing transcription [2]. In general, histone acetylation activity is correlated with transcriptional activation, whereas deacetylase activity is correlated with transcriptional repression. Global changes in gene expression are thought to result from the dynamic equilibrium between histone acetyl transferase ('HAT') enzyme activity and histone deacetylase (HDAC) enzyme activity within the nucleus of a cell.

HDACs mediate transcriptional repression by interacting with larger multisubunit complexes. For example, a specific HDAC known as HDAC1 is known to bind the co-repressor Sin3, and HDAC1–Sin3 further associates with the silencing mediators N-CoR and SMRT [3]. N-CoR/SMRT–HDAC1 is then recruited by specific transcription factors bound to promoter elements within the nucleus. For example, the retinoblastoma (Rb) gene product recruits N-CoR/SMRT–HDAC1 to bind the transcription factor E2F to repress E2F-regulated promoters [4–6]. HDAC1–Sin3 also binds to, and mediates repression by, the MAD/MAX repressor heterodimer [7]. The histone deacetylation activity of HDAC1 is essential for this transcriptional repression [8].

A variety of compounds possessing HDAC inhibitory activity have been shown to lead to the hyperacetylation of histones; this modification is accompanied by cell-cycle arrest and terminal differentiation in a number of cell types. Sodium butyrate, a non-specific HDAC inhibitor, induces cell arrest and induces a differentiated phenotype in a number of cancer cells [9–13]. Like butyrate, the fungal toxin trichostatin A (TSA), a potent, specific and reversible HDAC inhibitor, has also been shown to induce cell-cycle arrest and/or differentiation in a variety of systems. A synthetic benzamide derivative (MS-27275) with HDAC inhibitory activity was described recently [14]. MS-27275 induces histone hyperacetylation and demonstrates efficacy in inhibiting tumour growth in tumour-bearing nude mice. Because of the ability of these inhibitors to induce cell-cycle arrest or differentiation, interest has grown in the use of HDAC inhibitors as a cancer therapy [15–26].

Several cDNA species encoding HDACs have been characterized. The first to be cloned was the yeast protein RPD3, which was first identified in genetic screens for transcriptional repressors [27]. Mammalian HDAC1 was cloned independently as the molecular target of Trapoxin [28]. HDAC1 was found to be an orthologue of yeast RPD3; both were shown to have HDAC activity *in vitro*. Three cDNA species, HDAC1, HDAC2 and HDAC3, encoding proteins homologous with RPD3 have been described [29–31]. All three have ubiquitous tissue distributions and their activities seem to overlap. So far, five *Saccharomyces cerevisiae* genes have been found that encode HDACs; the family has been divided into two classes based on sequence conservation and proposed biochemical function. *S. cerevisiae* Hos1, Hos2, Hos3 and RPD3, together with mammalian HDAC1, HDAC2 and HDAC3 comprise class 1. The second class consists of the yeast HDA1 and HDA3 and the recently identified human homologues HDAC4, HDAC5, HDAC6 and HDAC7 [31–33].

Here we report the cloning and complete nucleotide sequence of HDAC8, a gene that encodes a protein product with similarity to the RPD3 class (I) of HDACs. We present evidence that

Abbreviations used: EST, expressed sequence tag; HDAC, histone deacetylase; RT–PCR, reverse-transcriptase-mediated PCR; TSA, trichostatin A.

[1] To whom correspondence should be addressed (e-mail joseph_buggy@axyspharm.com).
[2] Present address: Structural Genomics, Inc., San Diego, CA, U.S.A.
[3] Present address: The Genomics Institute of the Novartis Research Foundation, San Diego, CA, U.S.A.

HDAC8 possesses HDAC activity on histone H4 peptide substrates as well as on core histones.

EXPERIMENTAL

Cell lines, transfections and protein blots

HeLa cells were grown in Dulbecco's modified Eagle's medium (Gibco) supplemented with 10% (v/v) fetal bovine serum, penicillin (50 i.u./ml) and streptomycin (50 μg/ml). *Spodoptera frugiperda* (Sf9) cells were grown in 60 mm tissue culture dishes in Grace's complete insect medium (Invitrogen) supplemented with 10% (v/v) fetal bovine serum. Cells (2×10^6) were seeded and transfected with 10 μg of plasmid DNA by using the Insectin-Plus lipid-mediated transfection system (Invitrogen). Cells were harvested 4 days after transfection and lysed in buffer [50 mM Tris/HCl (pH 7.5)/150 mM NaCl/1.0% (v/v) Nonidet P40 containing protease inhibitor cocktail (Boehringer Mannheim)]. For immunoprecipitation, lysates were first precleared for 2 h with 50 μl of Protein A–agarose at 4 °C, followed by incubation with FLAG (DYKDDDK; single-letter amino acid codes) M2 monoclonal antibody (Sigma) overnight at 4 °C. Immune complexes were captured with Protein A–agarose and centrifuged; pellets were washed in PBS and subjected to electrophoresis on a 4–20% (w/v) gradient polyacrylamide gel. The gel was transferred to a nylon membrane, blocked with 2.0% (v/v) milk, incubated with FLAG antibody in 2.0% milk for 3 h at 37 °C and washed three times in TBS; this was followed by incubation with goat anti-mouse secondary antibody conjugated with either horseradish peroxidase or alkaline phosphatase (Pierce).

Cloning of HDACs

A search of the GenBank database of expressed sequence tags (ESTs) with the NCI BLAST server revealed an EST (1721472; accession number AI159768) from a uterine library with similarity to the N-terminal portion of HDAC3. From this information a primer was designed (TGCGGAACGGTTTTA-AGCGGAAG) and a human uterus Marathon-Ready cDNA library (Clontech) was screened by PCR with an upstream oligonucleotide primer (AP1) that annealed to a sequence within the library vector. The PCR product encoding the full-length clone was subcloned into pCRII (Invitrogen) to generate clone pCRH7; this was sequenced. As a confirmation, full-length cDNA was isolated from a human uterine cDNA library by Genome Systems with the use of colony plaque hybridization and pCRH7 as a probe. To create pcDNAH7 and pIZH7, plasmid pCRH7 was amplified by PCR with oligonucleotide primers specific for the HDAC8 sequence and engineered to insert the FLAG epitope tag sequence at the C-terminus. This product was subcloned into pcDNA3.1 and pIZV5 (Invitrogen) respectively. To create plasmid pIZH7aa containing the H142A/H143A mutation, HDAC8 was amplified by PCR from pIZH7 with oligonucleotides designed with mismatched base pairs by using the technique of overlap extension (as described in [34]), subcloned into pIZV5 and sequenced. The full-length cDNA for HDAC1 was isolated by PCR from a human uterine cDNA library (Clontech) by using oligonucleotides specific for HDAC1. The 5′ primer introduced an *Eco*RI restriction site upstream of the HDAC1 sequence; the 3′ primer introduced a *Not*I restriction site as well as the FLAG epitope tag sequence in-frame with the HDAC1-coding region. This PCR product was subcloned into the expression vectors pcDNA3.1 and pIZV5 and was confirmed by DNA sequence analysis.

Tissue expression profiling

Multiple tissue Northern blot and human tumour cell blots were purchased from Clontech. HDAC8 probe was prepared by digesting pCRH7 with *Bst*XI, purifying the 556 bp product from a 1.0% (w/v) agarose gel, and radiolabelling it with [α-^{33}P]dCTP with the use of a random prime labelling kit (Stratagene). Hybridization was performed under conditions of high stringency with ExpressHyb (Clontech) at 68 °C. Hybridized blots were washed in several changes of $2 \times$ SSC/0.05% SDS (SSC is 0.15 M NaCl/0.015 M sodium citrate) at room temperature for 30 min, followed by two washes in $0.1 \times$ SSC/0.1% SDS at 50 °C for 45 min. The blot was exposed to film with an intensifying screen at -70 °C for 8 days.

Quantitative reverse-transcriptase-mediated PCR (RT–PCR) was performed with TaqMan technology. First-strand cDNA was purchased from Clontech and used without further treatment. PCR reactions (50 μl) were performed in a buffer containing 50 mM KCl, 10 mM Tris/HCl, 10 mM EDTA, 5 mM $MgCl_2$, 200 μM dATP, 200 μM dCTP, 200 μM dGTP, 400 μM dUTP, 300 μM forward primer, 300 μM reverse primer, 200 μM probe, 1.25 units of AmpliTaq Gold and 0.5 unit of uracil-N-glycosylase. Primers and probes were designed by using Primer Express (ABI-Perkin-Elmer) and were as follows: actin-forward, 5′-TCACCCACACTGTGCCCATCTACGA-3′; actin-reverse, 5′-CAGCGGAACCGCTCATTGCCAATGG-3′; actin-probe, 5′-(FAM)ATGCCC(TAMRA)CCCCCATGC-CATCCTGCGT-3′; HDAC-forward, 5′-ACGGGCCAGTAT-GGTGCAT-3′; HDAC-reverse, 5′-GCCCTCTTGGCTGACC-TTCT-3′; HDAC-probe, 5′-(FAM)TGCATAAGCAGATGA-GGATAGTTAAGCCTAAAGTGC(TAMRA)-3′. Thermal cycling was performed with an ABI-7700 under the following reaction conditions: 50 °C for 2 min, 95 °C for 10 min followed by 40 cycles of 95 °C for 15 s and 60 °C for 60 s. Results were calculated with the 'ΔΔCt' method described by Winer et al. [35].

Linkage analysis

Genebridge-4 (GB4) 91-sample human–hamster radiation hybrid (RH) panels were purchased from Research Genetics. RH-DNA (25 ng) was spotted from purchased plates into 96-well PCR trays and dried. PCR was performed in duplicate with 5 units of Gibco BRL *Taq* polymerase, 2.5 mM dNTPs, 10 μM forward primer, 5′-AGTCACCAGTTTGTAGGGCAGGAG-3′ and 10 μM reverse primer, 5′-CACCTCCCAGTCTGCTGATCAG-TA-3′, in a total volume of 25 μl per reaction. PCR cycle conditions performed in a MJ Research PTC-100 were as follows: 95 °C for 3 min, followed by 25 cycles of 94 °C for 30 s, 60 °C for

Figure 1 DNA sequence and predicted amino acid sequence of HDAC8

(**A**) The entire nucleotide sequence and the deduced amino acid sequence of the HDAC8 clone. (**B**) Sequence similarity between HDAC8, HDAC1, HDAC2 and HDAC3. Proteins were aligned by using CLUSTAL W alignment from the MacVector sequence analysis package. Identical and similar residues are boxed; residues that are identical in all four proteins are highlighted in bold.

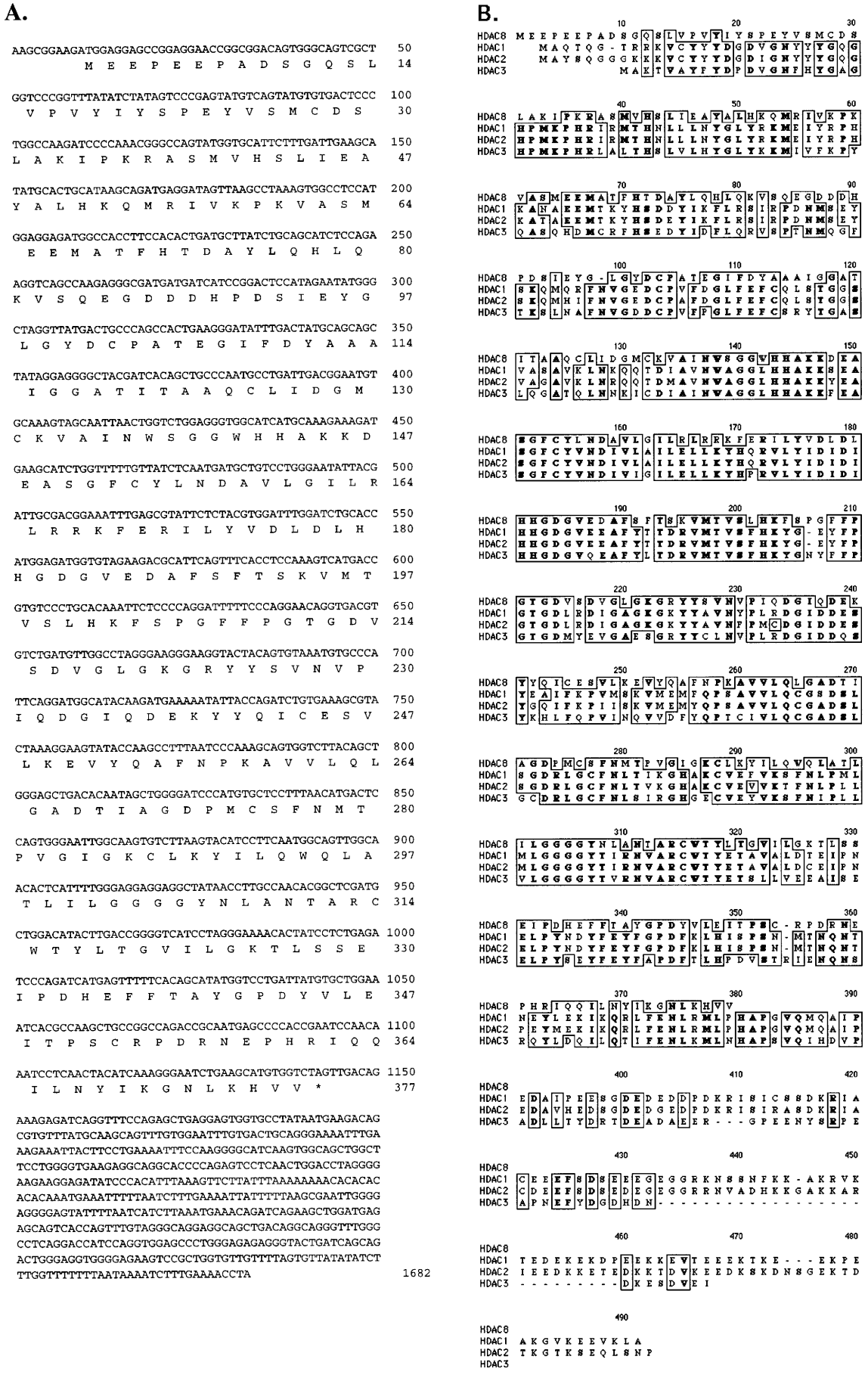

Figure 1 For legend see opposite page

30 s, 72 °C for 45 s, and then 72 °C for 1 min. This produced a product of 108 bp. PCR reactions were analysed by gel electrophoresis and scored 1 for duplicate reactions producing an identical PCR product, 0 for duplicate reactions with no PCR products produced, and 2 for any ambiguities between the two duplicate panels. Scored results were submitted via the Internet to the Whitehead Institute for Biomedical Research at MIT (http://www-genome.wi.mit.edu) and mapped relative to known sequence tagged sites.

Protein purification

Sf9 cells were lysed in lysis buffer [150 mM NaCl/50 mM Tris/HCl (pH 8.0)/1.0 % (v/v) Nonidet P40 containing protease inhibitor cocktail (Boehringer Mannheim)] and loaded on a G-25 (NP10) column. Proteins were eluted with 150 mM NaCl/50 mM Tris/HCl (pH 7.1) before being loaded on an anti-FLAG agarose-affinity column (Sigma). The column was washed extensively with wash buffer [150 mM NaCl/50 mM Tris/HCl (pH 7.1)/10 % (v/v) glycerol/0.5 % (v/v) Triton X-100] and proteins were eluted with 200 μg/ml FLAG peptide (Sigma) in wash buffer into 30 fractions of 200 μl, then assayed for activity and for expression by Western blot analysis.

Enzyme assays

HeLa cell immunoprecipitates were incubated with 20000 d.p.m. of [^{3}H]acetate-labelled peptide corresponding to the N-terminal 20 residues of human histone H4 (Upstate Biotechnology) for 2 h at 37 °C. FLAG-column-purified HDAC8 was incubated with 100000 d.p.m. of the [^{3}H]acetate-labelled H4 peptide for 4 h at 37 °C. The deacetylation reactions were performed in a buffer containing 10 mM Tris/HCl, pH 8.0, 125 mM NaCl and 10 % (v/v) glycerol. After extraction with ethyl acetate, released radioacetate was quantified with a β-scintillation counter (Wallac). Core histones from HeLa cells were prepared as described [36]. Anti-(acetyl-lysine) antibody was purchased from Upstate Biotechnology.

RESULTS

Cloning of a cDNA encoding a new HDAC

A search of the GenBank database of ESTs revealed an EST (1721472; accession number AI159768) from a uterine library with similarity to the N-terminal portion of HDAC3. To obtain a full-length clone, a uterine cDNA library was screened by using the technique of 3′-RACE (rapid amplification of cDNA ends). This technique yielded two distinct cDNA clones, one of 1.7 kb and one of 0.8 kb. Both fragment sizes were recovered with roughly the same frequency, suggesting that they were equally represented in the starting cDNA population. A sequence analysis of both forms demonstrated that the 0.8 kb transcript was identical with the 5′ end of the 1.7 kb transcript, corresponding to the N-terminal 146 residues. The origin of the truncated transcript is uncertain but it might represent an alternatively spliced product of the full-length mRNA or a cloning artifact present in the original cDNA library. The sequence of the 1.7 kb form (Figure 1A) predicts that this cDNA is a new member of the family of HDACs; it has been termed HDAC8.

The amino acid sequence of HDAC8 shares significant similarity with the HDAC class I enzymes as defined previously [31] (Figure 1B). Specifically, HDAC8 shares 30 % amino acid identity with HDAC1 and 31 % with HDAC2. HDAC8 is most similar to HDAC3, with 34 % amino acid identity and 54 % similarity, when one considers conservative amino acid substitutions. The predicted 377-residue product of the full-length HDAC8 cDNA clone contains a shorter C-terminal extension than other members of its class. In this respect HDAC8 is similar to the HDAC-like HDLP protein from *Aquifex aeolicus* whose crystal structure was reported recently [37]. Both HDAC8 and HDLP lack the approx. 100 C-terminal residues present in HDAC1, HDAC2 and HDAC3.

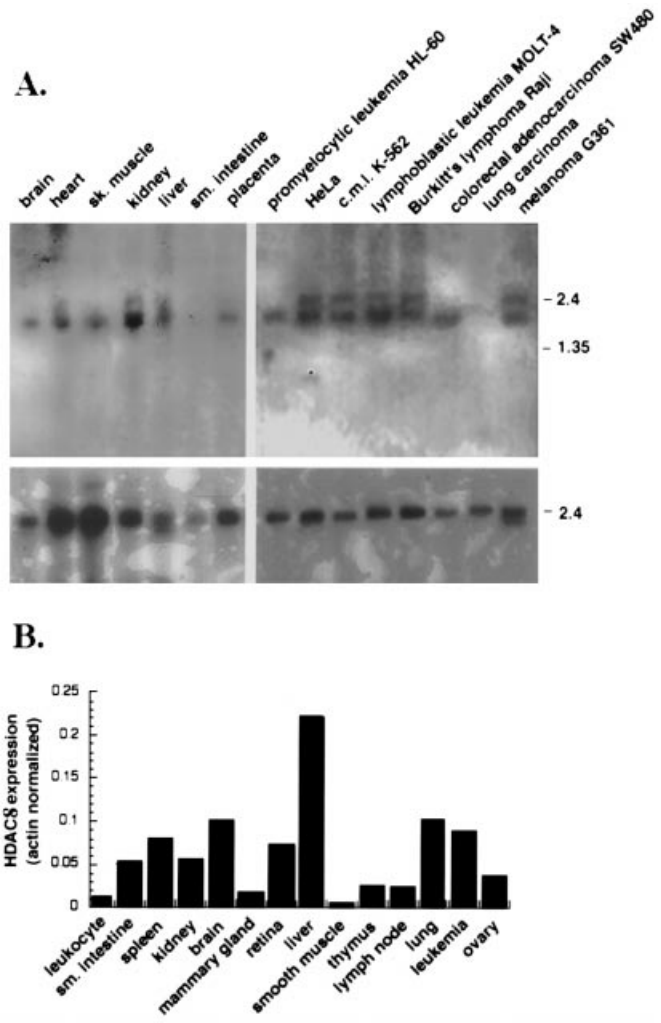

Figure 2 Expression of HDAC8 in various human tissues

(**A**) Northern blot analysis was performed on a multiple tissue blot and on tumour cell lines. Hybridization with ubiquitin is shown in the lower panels. (**B**) Quantitative RT–PCR was performed with TaqMan technology on various human cDNA species. Results shown are means for triplicate measures normalized with a standard actin probe.

Expression of HDAC8 in human tissues

To determine the transcript size of HDAC8, a human tissue blot and a human tumour cell blot were probed with a 556 bp *Bst*XI fragment representing nt 1–556 of HDAC8. As shown in Figure 2(A), a single major transcript of 1.7 kb was identified in several human tissues. A faint band of 2.4 kb could also be detected in the heart, kidney and liver lanes. The human tumour cell blot also revealed a transcript of 2.4 kb but in several tumour lines this larger transcript was observed to be of an intensity roughly equal to that of the 1.7 kb band. Subsequent cloning and sequence

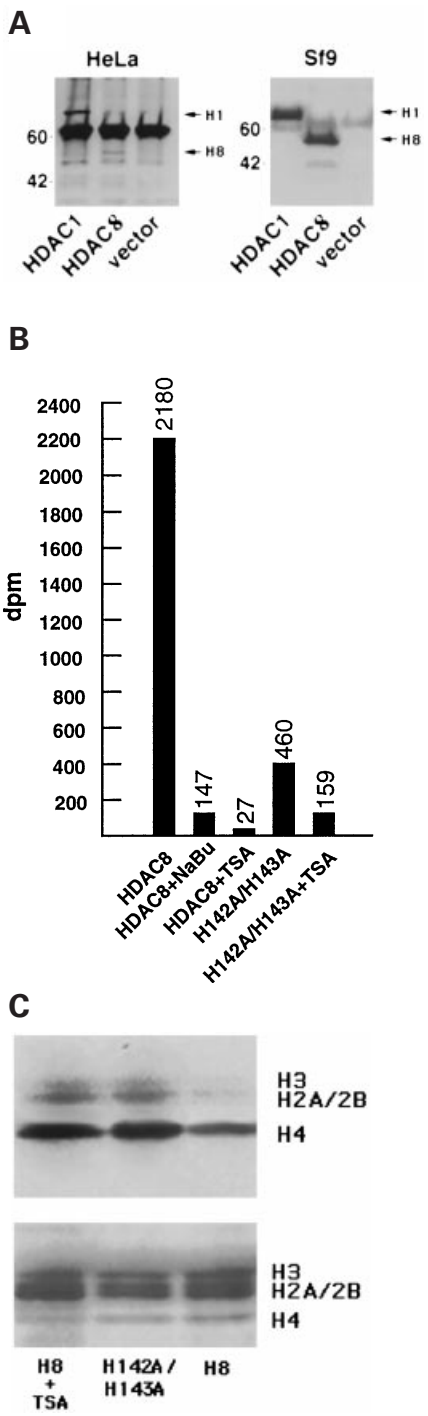

Figure 3 Activity of HDAC8

(**A**) Expression of HDAC1 and HDAC8 in HeLa and Sf9 cells. Cell lysates were immunoprecipitated with an anti-FLAG antibody and blotted with the same. Arrows indicate the positions of HDAC proteins. The positions of molecular mass markers are indicated (in kDa) at the left. (**B**) Activity of FLAG-column affinity-purified HDACs from transfected Sf9 cell lysates. A peptide corresponding to the N-terminal 20 residues of histone H4 was radioacetylated *in vitro* and used as a substrate for deacetylation. Results were normalized by subtracting data from untransfected cells. Numbers refer to averages for duplicate assays. (**C**) Deacetylation of core histones by HDAC8. Core histones (10 μg per lane) were separated by SDS/PAGE. The amount of protein in each lane is shown by Coomassie staining (lower panel). A Western blot of lanes probed with anti-(acetyl-lysine) is shown in the upper panel. Abbreviation: NaBu, sodium butyrate.

analysis of the 2.4 kb transcript from a HeLa cell cDNA library revealed that it encoded a product resulting in a fusion of 22 extraneous amino acid residues after Gly-234 of HDAC8, followed by a stop codon (results not shown). To compare differences in tissue expression more accurately from a wider range of tissues, real-time quantitative RT–PCR was performed on a number of human cDNA libraries by using TaqMan technology (Figure 2B). Every tissue examined contained detectable HDAC8 mRNA; the highest expression was found in liver.

Protein expression and HDAC activity of HDAC8

To examine the expression and activity of HDAC8 *in vitro*, FLAG-tagged HDAC8 and FLAG-tagged HDAC1 were transiently transfected into both HeLa cells and Sf9 insect cells. After the immunoprecipitation of cell lysates, expression of the enzymes was confirmed in both cell systems by Western blot analysis (Figure 3A). HDAC8 ran as a single band of 42 kDa in both systems. However, the apparent activity of HDAC8 immunoprecipitated from HeLa cell extracts was lower than that observed with HDAC8 immunoprecipitated from insect cell lysates, probably reflecting lower levels of protein expression in the HeLa system (Figure 3A, and results not shown). We therefore used the insect cell system to generate HDAC8 for further biochemical characterization. At 4 days after transfection with plasmid DNA encoding HDAC1, HDAC8 or empty vector, HDAC enzymes were partly purified from Sf9 cell lysates by passage over a FLAG affinity column. Fractions were eluted from the column with FLAG peptide and assayed for deacetylase activity on the radioacetylated H4 peptide substrate. As shown in Figure 3(B), HDAC8 deacetylated histone H4 in a reaction inhibited by both sodium butyrate (50 mM) and TSA (250 nM).

A previous study identified His-141 of HDAC1 as an important catalytic or structural residue of the enzyme [28]. Structural studies have predicted that both His-140 and His-141 form two independent hydrogen bonds essential for the Asp–His charge relay systems inherent in the active site [37]. To confirm the importance of these residues in HDAC8 catalysis, the homologous residues His-142 and His-143 were mutated to alanine. The H142A/H143A mutant was expressed with a FLAG tag in Sf9 cells concomitantly with wild-type HDAC8. Both proteins were partly purified over a FLAG affinity column; fractions determined by Western blot analysis to contain the protein were assayed for HDAC activity. As shown in Figure 3(B), mutant H142A/H143A lost more than 80% of its histone deacetylation activity relative to wild type. This demonstrates that one or both of these histidine residues is important in HDAC8 catalysis, presumably by participating in the Asp–His charge relay system of the active site.

To examine the substrate specificity of HDAC8 *in vitro*, acid-extracted histone proteins were incubated with HDAC8 and the acetylation state of each histone was determined. Western blot analysis with an antibody specific for *N*-acetyl-lysine demonstrated a significant reduction in acetylation of core histones H3 and H4 after incubation with HDAC8 (Figure 3C, upper panel). No such decrease in histone acetylation was seen when 300 nM TSA was included in the reaction. Deacetylation of the core histones by the H142A/H143A mutant was also significantly impaired. As a control for histone loading, the total protein in each lane was detected by running duplicate samples on the gel and staining with Coomassie Blue (Figure 3C, lower panel). As a further enzyme characterization, HDAC8 was incubated with various concentrations of TSA and sodium butyrate, and activity on the histone H4 peptide substrate was measured. As shown in

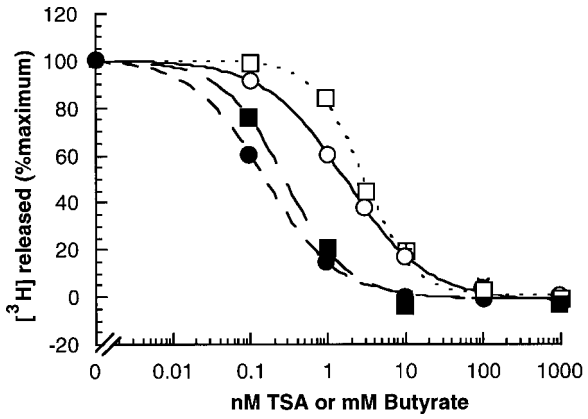

Figure 4 Inhibition of HDAC1, HDAC8, and H142A/H143A by TSA and sodium butyrate

FLAG-column-purified HDACs were incubated in the presence of increasing amounts of TSA or sodium butyrate. Symbols: □, HDAC8 + TSA; ○, HDAC1 + TSA; ■, HDAC8 + butyrate; ●, HDAC1 + butyrate. Results are expressed as percentages of the activity obtained in the absence of inhibitor.

Figure 4, HDAC8 activity was inhibited by both TSA and sodium butyrate with IC_{50} values similar to those obtained with HDAC1. The IC_{50} values for inhibition by TSA and butyrate were 3.0 nM and 0.35 mM respectively.

Chromosomal localization of HDAC8

To determine the physical location of HDAC8 in the human genome, we performed radiation hybrid (RH) mapping studies with oligonucleotides specific for the 3′ untranslated region of HDAC8. With the GB4 Whitehead-MIT (91 Hybrids) panel, HDAC8 was RH mapped to chromosome X relative to marker WI-1401 at Xq21.2. The Stanford G3 panel (89 Hybrids) also mapped HDAC8 to chromosome X relative to marker SHGC-16181 at Xq21.33. These results demonstrate that HDAC8 is a sex-linked gene residing at chromosomal position Xq21.2–q21.3.

DISCUSSION

We have cloned HDAC8, a novel deacetylase enzyme with similarity to the class I mammalian HDACs. HDAC8 shares the highest degree of sequence similarity to HDAC3, followed by HDAC2 and HDAC1 respectively. HDAC8 has an abbreviated C-terminus relative to HDAC1, HDAC2 and HDAC3. In this respect HDAC8 is similar to the HDLP protein from *A. aeolicus*, whose crystal structure was reported recently [37]. On the basis of the prediction of the crystal structure data, HDAC8 contains all of the residues of the active site including the two histidine residues (His-142 and His-143), two aspartic residues (Asp-176 and Asp-183) and one tyrosine residue (Tyr-306) predicted to participate in the charge-relay deacetylation mechanism. In addition, all of the residues predicted to co-ordinate Zn^{2+} near the bottom of the pocket are conserved between HDAC8, HDAC1 and HDLP, as are four out of six residues predicted to cover the walls of the active-site pocket.

We have detected the expression of HDAC8 in every tissue tested. Northern blot analysis revealed two transcripts: a major band of 1.7 kb and a second band of 2.4 kb that was especially prominent in several tumour lines. This larger transcript might have arisen as a result of alternative splicing and could potentially encode a form of HDAC8 that is truncated after Gly-234. Truncation at this position would delete many of the residues predicted to be important for HDAC enzyme activity and would presumably eliminate deacetylase activity. However, in the absence of evidence that this transcript is actually translated into protein, its relevance to HDAC and/or tumour biology is not clear. To quantify HDAC8 levels and compare various tissues, real-time quantitative RT–PCR was performed with Taqman technology. This method quantifies transcript levels on the basis of the number of amplification cycles necessary to produce a quantifiable product. Transcript levels from different tissues are normalized for actin abundance in each round of triplicate PCR cycles and can be directly compared on this basis. Although the 1.7 kb band seen in the kidney lane of the Northern blot is the most intense in comparison with those of the other tissues, the Taqman results demonstrate that HDAC8 expression is highest in liver.

We expressed HDAC8 and HDAC1 under the control of a cytomegalovirus promoter in two eukaryotic expression systems. The expression of recombinant HDAC8 in HeLa cells was low compared with that of recombinant HDAC1; it also seemed to be low relative to HDAC8 expression in insect cells. Interestingly, we were unable to derive stable HeLa cell lines overexpressing HDAC8, despite repeated attempts. It might be that the overexpression of HDAC8 is growth inhibitory or cytotoxic to mammalian cells. Because the expression of recombinant HDAC8 was significantly higher in insect cells, we used this system to produce partly purified enzyme for biochemical studies. HDAC8 deacetylated an acetylated peptide derived from histone H4 in a reaction that was inhibited by both sodium butyrate and TSA. HDAC8 was also able to deacetylate all core histones *in vitro*. In these respects HDAC8 is similar to all previously characterized HDACs. Site-directed mutagenesis of two conserved, tandem histidine residues within HDAC8 (H142A, H143A) significantly decreased, but did not abolish, the activity of the enzyme against both the H4 peptide and the core histone substrates. Previous reports have demonstrated the importance of the corresponding histidine residues for catalytic function in HDAC1 [28] and for the structural integrity of the active site of a related enzyme [28,37]. Our results are consistent with these findings and support the proposed role of these residues in the Asp/His charge relay mechanism of protein deacetylation.

In co-immunoprecipitation studies we were unable to detect a molecular interaction between HDAC8 and other characterized HDAC transcriptional cofactors such as YY1, mSin3a and RbAp48 (results not shown). HDAC8 activity might be regulated in a temporal or compartment-specific manner and/or have a more generalized role in transcriptional regulation. HDAC8 maps to the X chromosome at position Xq21.2–Xq21.3. The other class I deacetylases, HDAC1, HDAC2 and HDAC3, map to chromosomal positions 1p34, 6q21 and 5q31 respectively [38,39], making HDAC8 the only known example of an X-linked deacetylase. It is interesting to note that the inactive X chromosome in female mammals is distinguished by a lack of histone H4 acetylation, and hypoacetylation of specific promoters has been shown to be essential for X-inactivation [40–42]. Genetic deletions and insertions that encompass Xq21 have been identified that result in a randomized pattern of X-chromosome inactivation in tissues from affected individuals [43,44]. However, any specific role for HDAC8 in X-chromosome inactivation must be considered highly speculative at present.

REFERENCES

1 Grunstein, M. (1997) Histone acetylation in chromatin structure and transcription. Nature (London) **389**, 349–352

2 Walia, H., Chen, H. Y., Sun, J., Holth, L. T. and Davie, J. R. (1998) Histone acetylation is required to maintain the unfolded nucleosome structure associated with transcribing DNA. J. Biol. Chem. **273**, 14516–14522

3 Alland, L., Muhle, R., Hou, H., Potes, J., Chin, L., Schreiber-Agus, N. and DePinho, R. A. (1997) Role for N-CoR and histone deacetylase in Sin3-mediated transcriptional repression. Nature (London) **387**, 49–55

4 Luo, R. X., Postigo, A. A. and Dean, D. C. (1998) Rb interacts with histone deacetylase to repress transcription. Cell **92**, 463–473

5 Brehm, A., Miska, E. A., McCance, D. J., Reid, J. L., Bannister, A. J. and Kouzarides, T. (1998) Retinoblastoma protein recruits histone deacetylase to repress transcription. Nature (London) **391**, 597–600

6 Magnaghi-Jaulin, L., Groisman, R., Naguibneva, I., Robin, P., Lorain, S., LeVillain, J. P., Troalen, F., Trouche, D. and Harel-Bellan, A. (1998) Retinoblastoma protein represses transcription by recruiting a histone deacetylase. Nature (London) **391**, 601–605

7 Laherty, C. D., Yang, W. M., Sun, J. M., Davie, J. R., Seto, E. and Eisenman, R. N. (1997) Histone deacetylases associated with the mSin3 corepressor mediate mad transcriptional repression. Cell **89**, 349–356

8 Hassig, C. A., Tong, J. K., Fleischer, T. C., Owa, T., Grable, P. G., Ayer, D. E. and Schreiber, S. L. (1998) A role for histone deacetylase activity in HDAC1-mediated transcriptional repression. Proc. Natl. Acad. Sci. U.S.A. **95**, 3519–3524

9 Cioe, L., McNab, A., Hubbell, H. R., Meo, P., Curtis, P. and Rovera, G. (1981) Differential expression of the globin genes in human leukemia K562(S) cells induced to differentiate by hemin or butyric acid. Cancer Res. **41**, 237–243

10 Hoessly, M. C., Rossi, R. M. and Fischkoff, S. A. (1989) Factors responsible for variable reported lineages of HL-60 cells induced to mature with butyric acid. Cancer Res. **49**, 3594–3597

11 Kim, Y. S., Tsao, D., Diddiqui, B., Whitehead, J. S., Arnstein, P., Bennet, J. and Hicks, J. (1980) Effects of sodium butyrate and dimethylsulfoxide on biochemical properties of human colon cancer cells. Cancer **45**, 1185–1192

12 Ryan, M. P., Borenfreund, E. and Higgins, P. J. (1987) Butyrate-induced cytoarchitectural reorganization of Mallory body-containing rat hepatic tumor cells. J. Natl. Cancer Inst. **79**, 555–567

13 Graham, K. A. and Buick, R. N. (1988) Sodium butyrate induces differentiation in breast cancer cell lines expressing the estrogen receptor. J. Cell. Physiol. **136**, 63–71

14 Saito, A., Yamashita, T., Mariko, Y., Nosaka, Y., Tsuchiya, K., Ando, T., Suzuki, T., Tsuruo, T. and Nakanishi, O. (1999) A synthetic inhibitor of histone deacetylase, MS-27–275, with marked *in vivo* antitumor activity against human tumors. Proc. Natl. Acad. Sci. U.S.A. **96**, 4592–4597

15 Lin, R. J., Nagy, L., Inoue, S., Shao, W., Miller, W. H. and Evans, R. M. (1998) Role of the histone deacetylase complex in acute promyelocytic leukaemia. Nature (London) **391**, 811–814

16 Grignani, F., De Matteis, S., Nervi, C., Tomassoni, L., Gelmetti, V., Cioce, M., Fanelli, M., Ruthardt, M., Ferrara, F. F., Zamir, I. et al. (1998) Fusion proteins of the retinoic acid receptor-alpha recruit histone deacetylase in promyelocytic leukaemia. Nature (London) **391**, 815–818

17 Warrell, R. P., He, L. Z., Richon, V., Calleja, E. and Pandolfi, P. P. (1998) Therapeutic targeting of transcription in acute promyelocytic leukemia by use of an inhibitor of histone deacetylase. J. Natl. Cancer Inst. **90**, 1621–1625

18 Gelmetti, V., Zhang, J., Fanelli, M., Minucci, S., Pelicci, P. G. and Lazar, M. A. (1998) Aberrant recruitment of the nuclear receptor corepressor–histone deacetylase complex by the acute myeloid leukemia fusion partner ETO. Mol. Cell. Biol. **18**, 7185–7191

19 Wang, J., Hoshino, T., Redner, R. L., Kajigaya, S. and Liu, J. M. (1998) ETO, fusion partner in t(8;21) acute myeloid leukemia, represses transcription by interaction with the human N-CoR/mSin3/HDAC1 complex. Proc. Natl. Acad. Sci. U.S.A. **95**, 10860–10865

20 Archer, S. Y., Meng, S., Shei, A. and Hodin, R. A. (1998) p21(WAF1) is required for butyrate-mediated growth inhibition of human colon cancer cells. Proc. Natl. Acad. Sci. U.S.A. **95**, 6791–6796

21 Gillenwater, A., Xu, X. C., Estrov, Y., Sacks, P. G., Lotan, D. and Lotan, R. (1998) Modulation of galectin-1 content in human head and neck squamous carcinoma cells by sodium butyrate. Int. J. Cancer **75**, 217–224

22 Saunders, N., Dicker, A., Popa, C., Jones, S. and Dahler, A. (1999) Histone deacetylase inhibitors as potential anti-skin cancer agents. Cancer Res. **59**, 399–404

23 McBain, J. A., Eastman, A., Nobel, C. S. and Mueller, G. C. (1997) Apoptotic death in adenocarcinoma cell lines induced by butyrate and other histone deacetylase inhibitors. Biochem. Pharmacol. **53**, 1357–1368

24 Swendeman, S., Coffey, D. C., Rifkind, R. A., Marks, P. A., Richon, V. M. and La Quaglia, M. P. (1999) Hybrid polar histone deacetylase inhibitor induces apoptosis and CD95/CD95 ligand expression in human neuroblastoma. Proc. Am. Assoc. Cancer Res. **40**, Abstr. no. 3836

25 Yarden, R. I. and Brody, L. C. (1999) BRCA1 interacts with components of the histone deacetylase complex. Proc. Am. Assoc. Cancer Res. **40**, Abstr. no. 3387

26 Bakin, A. V. and Curran, T. (1999) Role of DNA 5-methylcytosine transferase in cell transformation by fos. Science **283**, 387–390

27 Vidal, M. and Gaber, R. F. (1991) RPD3 encodes a second factor required to achieve maximum positive and negative transcriptional states in *Saccharomyces cerevisiae*. Mol. Cell. Biol. **11**, 6317–6327

28 Taunton, J., Hassig, C. A. and Schreiber, S. L. (1996) A mammalian histone deacetylase related to the yeast transcriptional regulator Rpd3p. Science **272**, 408–411

29 Yang, W., Yao, Y., Sun, J., Davie, J. R. and Seto, E. (1997) Isolation and characterization of cDNAs corresponding to an additional member of the human histone deacetylase family. J. Biol. Chem. **272**, 28001–28007

30 Emiliani, S., Fischle, W., Van Lint, C., Al-Abed, Y. and Verdin, E. (1998) Characterization of a human RPD3 ortholog, HDAC3. Proc. Natl. Acad. Sci. U.S.A. **95**, 2795–2800

31 Grozinger, C. M., Hassig, C. A. and Schreiber, S. L. (1999) Three proteins define a class of human histone deacetylases related to yeast Hda1p. Proc. Natl. Acad. Sci. U.S.A. **96**, 4868–4873

32 Fischle, W., Emiliani, S., Hendzel, M. J., Nagase, T., Nomura, N., Voelter, W. and Verdin, E. (1999) A new family of human histone deacetylases related to *Saccharomyces cerevisiae* HDA1p. J. Biol. Chem. **274**, 11713–11720

33 Kao, H., Downes, M., Ordentlich, P. and Evans, R. M. (2000) Isolation of a novel histone deacetylase reveals that class I and class II deacetylases promote SMRT-mediated repression. Genes Dev. **14**, 55–66

34 Horton, R. M., Cai, Z, Ho, S. and Pease, L. R. (1990) Gene splicing by overlap extension: tailor-made genes using the polymerase chain reaction. Biotechniques **8**, 528–535

35 Winer, J., Jung, C. K., Shackel, I. and Williams, P. M. (1999) Development and validation of real-time quantitative reverse transcriptase–polymerase chain reaction for monitoring gene expression in cardiac myocytes *in vitro*. Anal. Biochem. **270**, 41–49

36 Carmen, A. A., Rundlett, S. E. and Grunstein, M. (1996) HDA1 and HDA3 are components of a yeast histone deacetylase (HDA) complex. J. Biol. Chem. **271**, 15837–15844

37 Finnin, M. S., Donigian, J. R., Cohen, A., Richon, V. M., Rifkind, R. A., Marks, P. A., Breslow, R. and Pavietich, N. P. (1999) Structures of a histone deacetylase homologue bound to the TSA and SAHA inhibitors. Nature (London) **401**, 188–193

38 Mahlknecht, U., Emiliani, S., Najfeld, V., Young, S. and Verdin, E. (1999) Genomic organization and chromosomal localization of the human histone deacetylase 3 gene. Genomics **56**, 197–202

39 Betz, R., Gray, S. G., Ekstrom, C., Larsson, C. and Ekstrom, T. J. (1998) Human histone deacetylase 2, HDAC2 (Human RPD3), is localized to 6q21 by radiation hybrid mapping. Genomics **52**, 245–245

40 Wakefield, M. J., Keohane, A. M., Turner, B. M. and Graves, J. A. (1997) Histone underacetylation is an ancient component of mammalian X chromosome inactivation. Proc. Natl. Acad. Sci. U.S.A. **94**, 9665–9668

41 Gilbert, S. L. and Sharp, P. A. (1999) Promoter specific hypoacetylation of X-inactivated genes. Proc. Natl. Acad. Sci. U.S.A. **96**, 13825–13830

42 O'Neill, L. P., Keohane, A. M., Lavender, J. S., McCabe, V., Heard, E., Avner, P., Brockdorff, N. and Turner, B. M. (1999) A developmental switch in H4 acetylation upstream of Xist plays a role in X chromosome inactivation. EMBO J. **18**, 2897–2970

43 Migeon, B. R., Stetten, G., Tuck-Muller, C., Axelman, J., Jani, M. and Dungy, D. (1995) Molecular characterization of a deleted X chromosome (Xq13.3–Xq21.31) exhibiting random X inactivation. Somat. Cell Mol. Genet. **21**, 113–120

44 Vust, A., Riordan, D., Wickstrom, D., Chudley, A. E. and Dawson, A. J. (1998) Functional mosaic trisomy of 1q12 → 1q21 resulting from X-autosome insertion translocation with random inactivation. Clin. Genet. **54**, 70–73

Received 20 March 2000/3 May 2000; accepted 26 May 2000